Linear Viscoelastic Behavior of Symmetric and Asymmetric Star Polymer Solutions

Jung Hun Lee,[†] Justin M. Goldberg,[‡] Lewis J. Fetters,[†] and Lynden A. Archer*,[†]

School of Chemical and Biomolecular Engineering, Cornell University, Ithaca, New York 14853, and Department of Chemistry and Chemical Biology, Cornell University, Ithaca, New York 14853

Received May 22, 2006; Revised Manuscript Received June 26, 2006

ABSTRACT: Linear viscoelastic properties of linear and star-branched polymer solutions are investigated experimentally and theoretically. Two series of high molar mass 1,4-polyisoprene linear and three-arm star polymers blended with marginally unentangled linear chains of the same chemistry form the focus of this study. We find that, irrespective of polymer architecture, unentangled linear molecules dilate the entanglement environment in the blends in a manner consistent with expectations for a Θ-solvent. A tube model analysis used in an earlier study [Lee, J. H.; Fetters, L. J.; Archer, L. A. *Macromolecules* **2005**, *38*, 4484], for predicting linear viscoelastic properties of branched melts, is extended to describe relaxation dynamics of entangled star-branched polymer solutions. We find that, by simply rescaling the model parameters to account for Θ-solvent dilution effects, this model quantitatively describes relaxation dynamics in concentrated star and linear polymer solutions, without adjustable parameters. At lower polymer concentrations, however, the tube model systematically overestimates the effect of solvent dilution on the dynamic moduli. These observations are discussed in terms of the universality of the dilution exponent and breakdown of dynamic dilution at low degrees of arm entanglement.

1. Introduction

In a previous article,[1] linear viscoelastic responses of a series of 1,4-polyisoprene asymmetric three-arm star polymers (A_2B) were studied by small-amplitude oscillatory shear measurements and a tube model theory in order to investigate branch-point motion of *hierarchically* relaxing polymer molecules. The number of entanglements formed by the short arm (B) was fixed at $M_B/M_e \sim 7$ to remove any ambiguity about its entanglement state, while the molecular weight of the long arms, M_A, was systematically varied from $7M_e$ to $43M_e$ in order to examine its effect on stress relaxation. Here $M_e = m_0N_e$ is the entanglement molecular weight; m_0 is the molecular weight of a Kuhn step. From a geometric viewpoint, one might naively anticipate that as M_A is systematically increased relative to M_B, initial starlike stress relaxation dynamics of asymmetric star polymers would give way to linearlike behavior. This expectation is in fact rigorously consistent with theories for entangled polymer relaxation based on the idea that branched molecules relax hierarchically and that the relaxed sections merely act to renormalize the tube friction coefficient of the unrelaxed component. Surprisingly, we found that, irrespective of the value of M_A/M_B, relaxation dynamics of asymmetric star polymer melts are qualitatively starlike over much of the time range accessed by rheological experiments.

To explain this observation, Lee et al. proposed a mechanism wherein on time scales longer than the relaxation time of the arms the tube diffusion coefficient, D_{eff}, of the linearlike polymer backbone is substantially smaller than anticipated under the simple hierarchical relaxation assumption. These authors in fact proposed that D_{eff} is an explicit function of the number of short arm entanglements.[1] Significantly, when the proposed mechanism is introduced to the tube model for branched polymers proposed by McLeish and co-workers,[2−5] it yields a self-consistent theory for the linear viscoelasticity (LVE) of all entangled homopolymers (linear and branched).[1] In a series of two papers we evaluated predictions based on this model using published experimental data from many groups. It was found that predictions of the theory are in essentially quantitative accord with all published data for asymmetric star polymer melts[1] as well as for branched polymer melts with more complex architectures (H-shaped, combs, pom-poms, etc.).[6] A key assumption of this model is that the branch point of all branched molecules is constrained to move in a tube of diameter $a_0 \approx \sqrt{N_e}b$, i.e., the undilated or bare tube diameter. This assumption is controversial because it disagrees with the basic premise of the dynamic dilution model, namely that the tube environment in which branched molecules diffuse is continuously dilated by relaxed portions of the same molecules.[2,7,8] Recent diffusion studies using symmetric star polymers, nonetheless, show that the product of the self-diffusion coefficient and zero-shear viscosity are in better agreement with the theoretical estimate based on branch-point motion in an undilated tube.[9,10] However, it remains a matter of debate whether the systems used in these studies span a wide enough range of arm entanglements to conclusively prove that branch-point motion is in fact constrained to the undilated tube.

Stress relaxation measurements using entangled solutions of branched polymers provide a ready means (by solvent dilution) of extending the range of arm entanglement densities explored, making it possible to study the role of the these entanglements on branch-point motion and stress relaxation dynamics in detail. Solution studies of well-characterized branched molecules are nonetheless surprisingly rare. Daniels et al.,[11] for example, prepared 50% solutions of linear, star-shaped, and H-shaped polyisoprene polymers in squalane. Relaxation responses of melts and solutions were compared with predictions of a hierarchical tube model theory with their melt entanglement molecular weight M_e and plateau modulus G_N rescaled to the respective Θ-solvent values, $M_e(\phi_p) \sim M_e\,\phi_p^{-4/3}$ and $G_N(\phi_p) \sim G_N\,\phi_p^{7/3}$, where ϕ_p is the volume fraction of polymer in solution. Daniels et al. found that an empirical form of the entanglement

[†] School of Chemical and Biomolecular Engineering.
[‡] Department of Chemistry and Chemical Biology.

10.1021/ma061151a CCC: $33.50
Published on Web 08/23/2006

jump time, $\tau_e(\phi_p) \sim \tau_e\phi_p^{-2.04}$, was required to reproduce the measured relaxation spectrum over the widest frequency range. It is noteworthy that the entanglement equilibration time is expected as $\tau_e(\phi_p) \sim \phi_p^{-5/3}$ for Θ-solvent theory,[12,13] while the relationship $M_e(\phi_p) = M_e/\phi^{4/3}$ leads to $\tau_e(\phi_p) = \tau_e[M_e(\phi_p)/M_e]^2 \sim \phi_p^{-8/3}$.

Miros et al.[14] investigated relaxation behavior of a series of 1,4-polybutadiene multiarm star solutions with large number of arms ($f > 56$) per branch point dissolved in oligomeric linear polybutadiene chains. The authors showed that the tube model with dynamic dilution and Θ-solvent scalings correctly captures the primary arm retraction processes in these materials but could not describe their slow terminal relaxation behavior, thought to originate from the star's colloidal core. In this case, however, values of $\tau_e(\phi_p)$ used for the tube model predictions do not obey either of the usual formulas, $\tau_e(\phi_p) = \tau_e\phi_p^{-5/3}$ or $\tau_e(\phi_p) = \tau_e\phi_p^{-8/3}$.

Finally, Juliani and Archer[15] recently reported linear and nonlinear viscoelasticity of 1,4-polybutadiene multiarm polymer ($A_3\mathbf{A}A_3$) solutions. By systematically changing the arm (A) entanglement density through dilution by an unentangled linear 1,4-polybutadiene oligomer, these authors were able to probe material properties ranging from starlike to linearlike, for a range of backbone **A** molecular weights. Significantly, the authors found that as the degree of solvent dilution increases, terminal relaxation of these solutions become substantially slower than predictions based on the H-polymer theory with $M_e(\phi_p) = M_e/\phi_p^{4/3}$. A more recent theoretical study of $A_3\mathbf{A}A_3$ polymer solutions by Archer and Juliani[16] showed the backbone dynamics are slowed by an amount proportional to the dilated tube diameter of the solutions. These authors also found that an additional empirical, concentration-dependent fitting parameter, p^2, was required to correctly predict the low-frequency (long-time) dynamics of entangled pom-pom solutions.

In this article we investigate stress relaxation dynamics in entangled solutions of starlike polymers. Our specific focus is on three-arm symmetric (S) and asymmetric (A_2B) star polyisoprenes dissolved in an unentangled linear isoprene oligomer. Given the success of the tube model theory introduced in refs 1 and 2, it is perhaps obvious to inquire about its suitability/limitations for describing dynamics in entangled branched polymer solutions. Systematic solution studies are also advantageous for evaluating the premise that relaxation dynamics of entangled melts are identical to those of their corresponding solutions, with $M_e(\phi_p) \sim \phi_p^{-\alpha}$, $G_N(\phi_p) \sim \phi_p^{1+\alpha}$, $\tau_e(\phi_p) = \tau_e[M_e(\phi_p)/M_e]^2 \sim \phi_p^{-2\alpha}$, and $\alpha = 4/3$. Provided the arm molecular weights are sufficiently high, $M_e(\phi_p)$ can be made arbitrarily large, allowing an extremely wide range of tube diameters to be sampled. This last feature of branched solutions is important because it allows us to systematically test the limitations of the dilated vs undilated tube assumption with much greater specificity than possible with entangled melts.

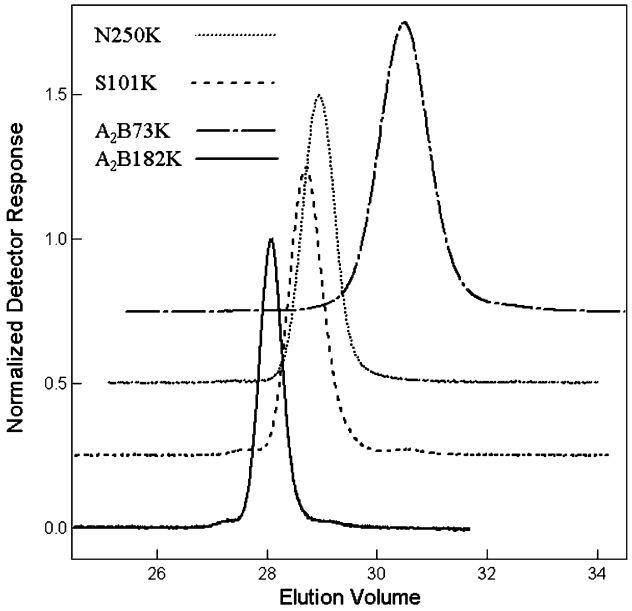

Figure 1. GPC analysis of 1,4-polyisoprene linear (N250K), three-arm symmetric star (S101K), and three-arm asymmetric star (A_2B73K and A_2B182K) polymers.

2. Experiment

A series of linear 1,4-polyisoprene linear (N), symmetric (S), and asymmetric star (A_2B) polymers were synthesized using anionic techniques under high-vacuum conditions. The detailed synthesis schemes and procedures for fractionating high-quality branched polymers are described in previous papers.[1,17] Molecular weights of all polymers used in this study were characterized using a Viscotek size-exclusion chromatograph (SEC) comprised of four mixed-bed columns and equipped with a laser light scattering detector (TDA 302). Figure 1 shows GPC traces of polymers used in this study. The microstructures of the polymers were characterized using ^{1}H NMR analysis.[18] Characterization results are provided in Table 1. 1,4-Polyisoprene linear (N250K), three-arm symmetric star (S101K), and three-arm asymmetric star (A_2B73K and A_2B182K) polymers were blended with short linear 1,4-polyisoprene

Table 1. Polymer Characterization

sample	M_n (SEC with LS) [g/mol] (1) short (2) long (3) total	PDI	microstructure by ^{1}H NMR [%] (1) cis-1,4 (2) trans-1,4 (3) 3,4	η_0 [Pa·s]	$\omega_{crossover}$ [1/s]	$\omega_{\eta''max}$ [1/s]	M in model [g/mol] (1) short (2) long
N4K	(1)		(1) 68.6				
	(2)		(2) 24.7				
	(3) 3220	1.11	(3) 6.7				
N250K	(1)		(1) 74.4				
	(2)		(2) 19.8	6.64×10^5	4.19×10^{-1}	3.16×10^{-1}	280000
	(3) 256900	1.01	(3) 5.8				
S101K	(1) 101000	1.01	(1) 75.7	1.36×10^7	6.29×10^{-3}	2.68×10^{-3}	(1) 101000
	(2)		(2) 19.2				
	(3) 299800	1.02	(3) 5.1				
A_2B73K	(1) 33000	1.01	(1) 71.5	2.91×10^5	5.75×10^{-1}	1.59×10^{-1}	(1) 33000
	(2) 73400	1.05	(2) 21.4				(2) 73400
	(3) 169000	1.06	(3) 7.1				
A_2B182K	(1) 33000	1.01	(1) 73.1	1.68×10^8	3.57×10^{-4}	2.28×10^{-4}	(1) 33000
	(2) 182000	1.06	(2) 18.9				(2) 182000
	(3) 370000	1.02	(3) 8.0				

Table 2. Linear Viscoelastic Properties

sample	$G_N(\phi_p)$ [Pa]	η_0 [Pa·s]	$\omega_{crossover}$ [1/s]	sample	$G_N(\phi_p)$ [Pa]	η_0 [Pa·s]	$\omega_{crossover}$ [1/s]
N250K80	2.73×10^5	2.51×10^5	6.49×10^{-1}	S101K80	2.78×10^5	1.67×10^6	4.55×10^{-2}
N250K70	2.00×10^5	1.15×10^5	1.05	S101K70	2.06×10^5	5.20×10^5	1.47×10^{-1}
N250K60	1.40×10^5	6.88×10^4	1.24	S101K60	1.47×10^5	1.94×10^5	3.39×10^{-1}
N250K50	9.29×10^4	3.46×10^4	1.69	S101K50	9.72×10^4	6.12×10^4	8.84×10^{-1}
N250K40	5.47×10^4	1.47×10^4	2.45	S101K40	5.44×10^4	1.58×10^4	2.40
N250K30	2.65×10^4	4.47×10^3	4.42	S101K30	2.72×10^4	4.66×10^3	5.31
N250K20	1.22×10^{4a}	1.10×10^3	8.76	S101K20	1.22×10^{4a}	6.65×10^2	1.73×10
A_2B73K80	2.61×10^5	6.00×10^4	2.25	A_2B182K80	2.88×10^5	2.15×10^7	1.98×10^{-3}
A_2B73K70	1.98×10^5	3.21×10^4	3.83	A_2B182K60	1.56×10^5	1.58×10^5	2.55×10^{-2}
A_2B73K60	1.34×10^5	1.36×10^4	7.23	A_2B182K20	1.36×10^{4a}	3.54×10^3	2.52
A_2B73K50	9.68×10^{4a}	4.55×10^3	1.56×10				

[a] Evaluated from the average storage modulus value where the minimum of tan(δ) is observed.

chains (N4K) at different weight fractions in excess cyclohexane. Following complete dissolution of polymers, cyclohexane was driven off in a vacuum oven at room temperature. For brevity, sample names are coded with the fraction of polymer melts. For example, A_2B73K80 refers to A_2B73K and N4K blend with 80 wt % of A_2B73K ($\phi_p = 0.8$).

Stress relaxation dynamics of linear, symmetric, and asymmetric star polymer solutions were quantified using small-amplitude oscillatory shear measurements. A Rheometric Scientific Inc. (RSI) ARES-LS rheometer with 4−12 mm diameter parallel-plate fixtures was used for all experiments reported in this article. Linear viscoelastic properties of all solutions were measured at temperatures ranging from −45 to 28 °C. The low-temperature experiments were performed with smaller diameter parallel-plate to reduce torque compliance during measurement. The RSI Ochestrator software was used to automatically derive master curves at a reference temperature $T_{ref} = 28$ °C by a two-dimensional residual minimization technique. The obtained linear viscoelastic properties of all samples are shown in Table 2. The plateau modulus $G_N(\phi_p)$ is evaluated from the average storage modulus values at which the loss minimum is observed, and the zero-shear viscosity $\eta_0(\phi_p) = G''(\omega)/\omega|_{\lim \omega \to 0}$ is obtained directly from the oscillatory shear data.

3. Results and Discussion

Dynamic storage and loss moduli, $G'(\omega)$ and $G''(\omega)$, over the entire frequency range are shown in Figure 2 for polymer solutions of different architectures at polymer concentrations $\phi_p = 0.8$ and 0.2. Several important features are apparent from the dynamic moduli of these solutions. First, as ϕ_p is decreased, the influence of solvent dilution on the relaxation dynamics of linear, symmetric, and asymmetric star polymers are seen to manifest primarily as reductions in the plateau modulus $G_N(\phi_p)$ and a leftward shift of the high-frequency $G'(\omega)-G''(\omega)$ crossover point. The changes in $G_N(\phi_p)$ is consistent with a loosening of the entanglement network, while the shift in the high-frequency $G'(\omega)-G''(\omega)$ crossover qualitatively indicates that the entanglement equilibration time $\tau_e(\phi_p)$ is significantly increased by solvent dilution. Second, it is apparent that the high-frequency $G'(\omega)-G''(\omega)$ crossover point is almost identical for all architectures at the same polymer concentration. This indicates that local motion of chain segments is not a function of architecture and is uniformly affected by the unentangled linear chains (solvent).

The existence of branching is clearly recognized from the different shapes of the $G''(\omega)$ peak at intermediate frequencies. For example, in solutions with $\phi_p = 0.8$, the magnitude of the maximum in $G''(\omega)$ of S101K80, A_2B75K80, and A_2B182K80 is seen to be substantially broader and lower than that of N250K80. This characteristic is consistent with the expectation from the arm retraction process. Such a distinctive branching effect in the $G''(\omega)$ peak, on the other hand, disappears in the relaxation spectrum of 20% solutions. The entanglement densities of the arm of S101K20 and the short arm of A_2B182K20

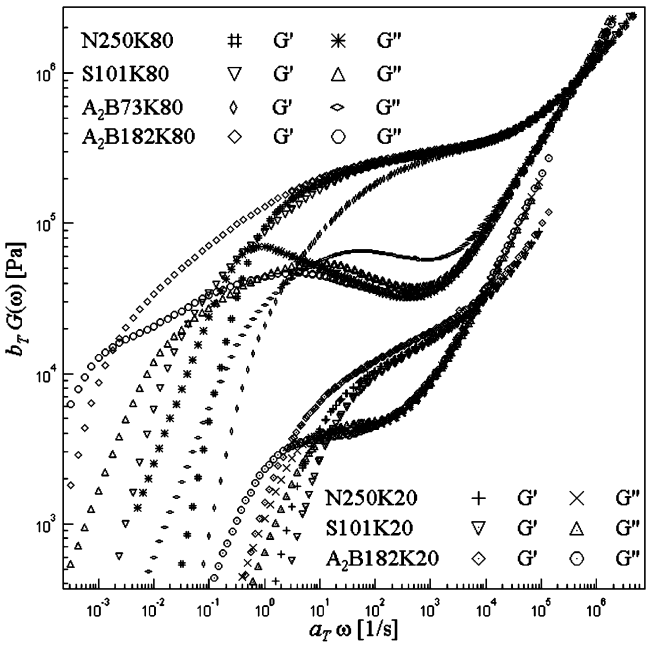

Figure 2. Dynamic moduli, $G'(\omega)$ and $G''(\omega)$, of 1,4-polyisoprene linear (N250K), three-arm symmetric star (S101K), and three-arm asymmetric star (A_2B73K and A_2B182K) polymer solutions with polymer concentrations $\phi_p = 0.8$ and 0.2. The reference temperature is $T_{ref} = 28$ °C.

become small enough to lessen the arm retraction process in these branched architectures. In an earlier study,[1] $M_e = 4004$ g/mol was obtained from the measured plateau modulus of the A_2B series polymer melts, while $M_{ef} = 4200$ g/mol was deduced from tube model fits of these data. Thus, for $\phi_p = 0.2$, the number of entanglements per arm is indeed close to the accepted lower bound for the entanglement effect $M_C/M_e = 2-3$, if $M_e(\phi_p) = M_e/\phi^{4/3}$ is used. Also, the terminal relaxation of S101K20 is observed to become faster than that of N250K20, which is also consistent with the transition to unentangled starlike dynamics at these low polymer concentrations. This observation can be contrasted with what is seen in S101K80, where a dominant arm retraction process is clearly evident into the terminal regime—again precisely what one would expect for an entangled star. Together these results indicate that the unentangled linear chains used here as solvent do in fact so act, regardless of the polymer architecture.

To quantify the effect of dilution on linear viscoelastic properties, values of the plateau modulus $G_N(\phi_p)$ and zero-shear viscosity $\eta_0(\phi_p)$ are plotted against ϕ_p in parts a and b of Figure 3, respectively. Here $G_N(\phi_p)$ is estimated as the storage modulus value corresponding to the loss minimum in the rubbery plateau regime. Figure 3a illustrates the dependence of $G_N(\phi_p)$ on the polymer concentration for linear, symmetric, and asymmetric

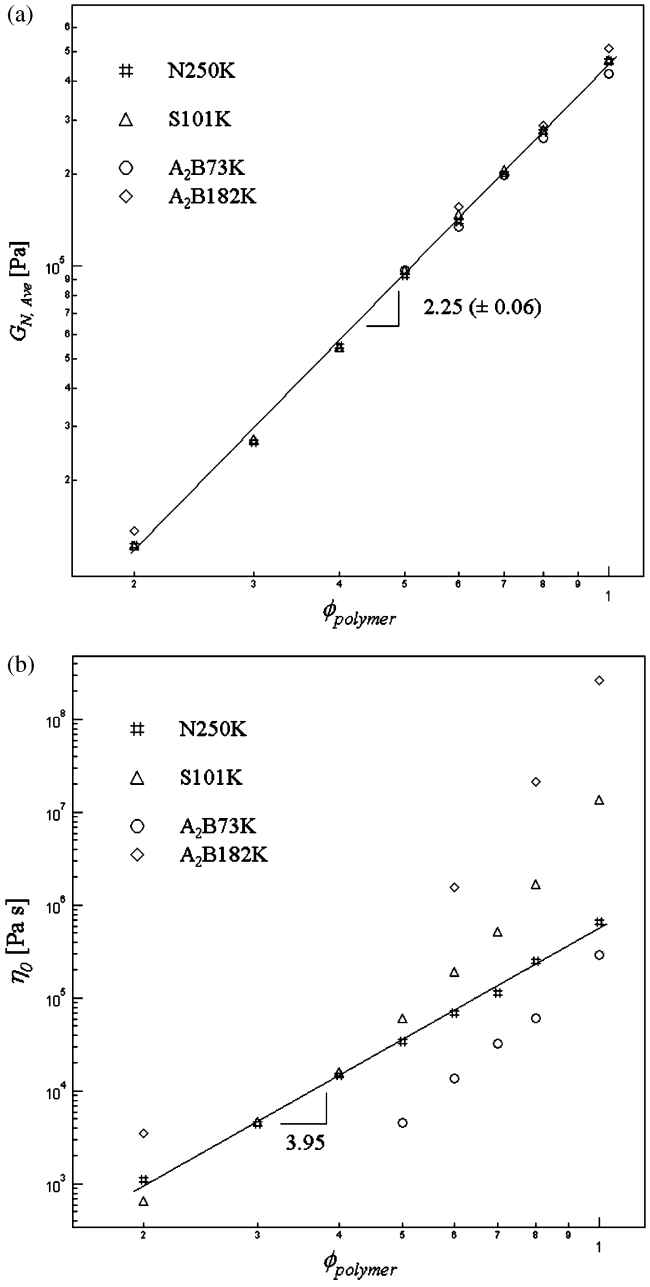

Figure 3. Concentration dependence of viscoelastic properties of 1,4-polyisoprene linear (N250K), three-arm symmetric star (S101K), and three-arm asymmetric star (A_2B73K and A_2B182K) polymer solutions: (a) the plateau modulus $G_N(\phi_p)$ vs ϕ_p and (b) the zero-shear viscosity $\eta_0(\phi_p)$ vs ϕ_p.

star structures. The slope 2.25 ± 0.06 from a series of solutions is very close to the expectation from the Θ-solvent or good-solvent scalings,[12,13,19] $G_N(\phi_p) \sim \phi_p^{\alpha+1}$ with $\alpha \approx 1.3$, within experimental error. On this basis as well as on the basis of the size and chemistry of N4K, one would conclude that the effect of dilution by N4K on the entanglement network is in essentially quantitative accord with expectations from the Θ-solvent exponent. On the other hand, the dependence of $\eta_0(\phi_p)$ on the polymer concentration in Figure 3b appears too complicated to quantify by a single scaling exponent, except for the N250K solutions. In this case the anticipated scaling for an ideal Θ-solvent[12,13] is $\eta_0(\phi_p) \sim \phi_p^{14/3 \approx 4.67}$, which is evidently stronger than the exponent of 3.95 deduced from the experimental data. The observed scaling is nonetheless consistent with the experimentally observed exponents in the range of 3.4−4 from linear

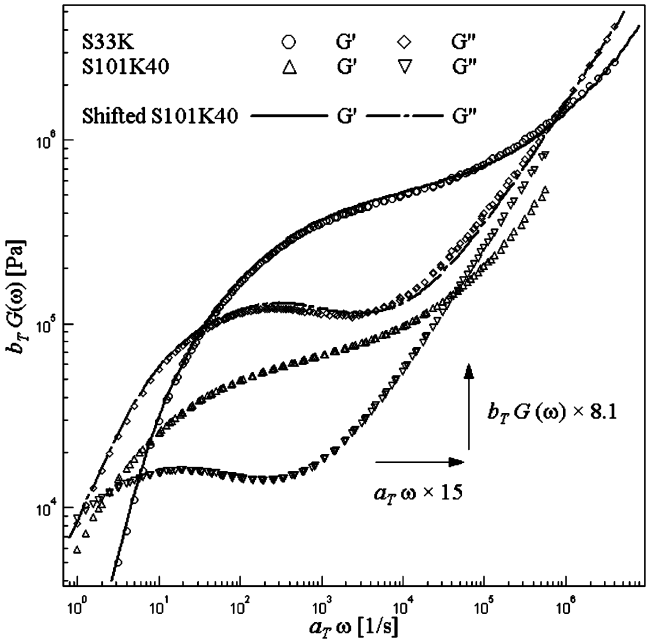

Figure 4. Dynamic moduli, $G'(\omega)$ and $G''(\omega)$, of 1,4-polyisoprene three-arm symmetric star polymer melts (S33K) and solutions (S101K40). The reference temperature is $T_{ref} = 28$ °C.

polymer solution studies using Θ-solvents or unentangled diluent chains of the same chemistry.[20−23]

To understand the deviations between the measured and predicted exponents for the zero-shear viscosity of N250K solutions, it is useful to write the zero-shear viscosity as $\eta_0(\phi_p) = G_N(\phi_p) \times \tau_{rep}(\phi_p)$. Writing $G_N(\phi_p) \sim \phi_p^{7/3}$ and $\tau_{rep}(\phi_p) = \tau_e(\phi_p)[M/M_e(\phi_p)]^{3.4} \sim \tau_e(\phi_p)\phi_p^{68/15}$, it is apparent that $\eta_0(\phi_p) = G_N\, \phi_p^{103/15}\tau_e(\phi_p)$. Thus, if $\eta_0(\phi_p) \sim \phi_p^{3.95}$, then $\tau_e(\phi_p) \sim \phi_p^{-2.92}$, which is closer to the prediction $\tau_e(\phi_p) = \tau_e[M_e(\phi_p)/M_e]^2 \sim \phi_p^{-8/3}$ than to the relation $\tau_e(\phi_p) \sim \phi_p^{-5/3}$ used in the earlier literature.[12,13] It is also of interest to determine whether the premise that relaxation dynamics of branched molecules in the melt are equivalent to those in solution provided the number of entanglements per chain are the same. A simple way to examine this effect is to compare relaxation moduli of symmetric star polymer melts with those of star polymer solutions with equivalent number of entanglements per arm. 1,4-Polyisoprene three-arm symmetric star polymers (S33K) with $M_{arm}/M_{ef} = 7.9$ (or $M_{arm}/M_e = 8.2$) were synthesized in the earlier study,[1,17] while S101K40 with N4K yields $M_{arm}/M_{ef}(\phi_p) = 7.1$ (or $M_{arm}/M_e(\phi_p) = 7.4$) per arm. Dynamic moduli of S101K40 are shifted vertically and horizontally in order to remove the effect of solvent dilution on the plateau modulus and entanglement equilibration time. This allows any differences between the linear viscoelastic responses of the two polymers to be easily observed. As seen in Figure 4, the shifted relaxation moduli of S101K40 overlap almost perfectly with the dynamic moduli of S33K over the entire frequency range, convincingly supporting the idea that relaxation dynamics in the two materials are equivalent and underscoring the importance of the degree of entanglement per arm as the variable that most significantly controls stress relaxation in entangled stars.

The results in Figure 4 also provide a method for independently checking the solution concentration or dilution exponent. Specifically, the dynamic moduli of S101K40 are vertically shifted by a factor 8.1, indicating that the effect of N4K on the entanglement network is given by the relation $G_{N,shifted} = G_N(\phi_p) \times 8.1$. This leads to $1/\phi_p^{1+\alpha} = 8.1$; the estimated polymer concentration is $\phi_{p^*} = (8.1)^{-1/[\alpha+1]} = 0.408$ if $\alpha = 4/3$, while

the estimated dilution exponent $\alpha^* = -[\log 8.1/\log 0.4] - 1 = 1.28$ if we take $\phi_p = 0.4$. Both results are consistent with the known volume fraction, $\phi_p = 0.4$, of stars in S101K40 and conform that N4K does indeed satisfy Θ-solvent-like scaling.

It is therefore possible to apply the tube model theory for branched polymer melts evaluated in refs 1 and 2 to any star polymer solution with the following definitions: $M_e(\phi_p) = M_e/\phi_p^{4/3}$, $\tau_e(\phi_p) = \tau_e[M_e(\phi_p)/M_e]^2 = \tau_e/\phi_p^{8/3}$, and $G_N(\phi_p) = G_N\phi_p^{\alpha+1}$. Here, as before, M_e, τ_e, and G_N are respectively the entanglement molecular weight, entanglement equilibration time, and plateau modulus in the melt. In the case of asymmetric star polymers, the number of entanglements per long arm $Z_{A,sol}$ and short arm $Z_{B,sol}$ is defined as $Z_{A,sol} = N_A/N_e(\phi_p) = [M_A/m_0]/[M_e(\phi_p)/m_0]$ and $Z_{B,sol} = N_B/N_e(\phi_p) = [M_B/m_0]/[M_e(\phi_p)/m_0]$, respectively. With the volume fraction ϕ_i and the fractional distance from the end of arm s_i with subscripts i indicating long arms (i = A) and short arms (i = B), the effective fraction of unrelaxed segments $\Phi(s_i) = \phi_p[\phi_A(1 - s_A) + \phi_B(1 - s_B)] = \phi_p[1 - g_i s_i]$ with g_i defined in ref 1 yields the effective potential $U_{eff,i}(s_i)$ for asymmetric star polymer solution as

$$\begin{aligned} d \ln \tau_i/ds_i &= \partial U(s_i,N_e(s_i))/\partial s_i = 3[N_i/N_e(\Phi(s_i))]s_i \\ &= 3[N_i/N_e]s_i\Phi(s_i)^\alpha = \partial U_{eff,i}(s_i)/\partial s_i \quad (1) \end{aligned}$$

$$\begin{aligned} U_{eff,i}(s_i) &= \int_0^{s_i} 3[N_i/N_e]s_i'[\phi_p(1 - g_i s_i')]^\alpha \, ds' \\ &= 3[N_i/N_e]\phi_p^\alpha \int_0^{s_i} s_i'[(1 - g_i s_i')]^\alpha \, ds' \\ &= 3Z_{i,sol}\frac{1 - (1 - g_i s_i)^{\alpha+1}[1 + (\alpha + 1)g_i s_i]}{g_i^2(\alpha + 1)(\alpha + 2)} \quad (2) \end{aligned}$$

Thus, Z_i and τ_e in eqs A-1 to A-6 of ref 1 are simply replaced by $Z_{i,sol}$ (e.g., equivalent to replacing M_e to $M_e(\phi_p)$) and $\tau_e(\phi_p)$. After the relaxation of the short arm $\tau_{a,B}$, the effective fraction of unrelaxed segments of remaining long arms reduces from $\Phi(\tau_{a,B}) = \Phi(s_{AR}) = \phi_p[\phi_B(1 - s_{AR}\sqrt{Z_{A,sol}/Z_{B,sol}}) + \phi_A(1 - s_{AR})]$ to $\phi_p\phi_A(1 - s_{AR}) = \phi_{Rbb}$ so that the constraint-release Rouse time τ_C is defined as $\tau_C = \tau_{a,B}[\Phi(\tau_{a,B})/\phi_{Rbb}]^{2\alpha}$. Therefore, any further relaxation after τ_C is specified in terms of the dilated entanglement molecular weight $M_e(\phi_p\phi_A) = M_e/(\phi_p\phi_A)^\alpha$ and the diluted entanglement equilibrium time $\tau_e(\phi_p\phi_A) = \tau_e/(\phi_p\phi_A)^{2\alpha}$. Thus, $Z_{A,D}$ and $\tau_{e,D}$ in eqs A-7 to A-9 of ref 1 are replaced $M_A/M_e(\phi_p\phi_A)$and $\tau_e(\phi_p\phi_A)$. Finally, the terminal relaxation time in the bare tube can be expressed as

$$\tau_d = 3\left(\frac{2N_{AR}}{N_e}\right)^3(1 - s_d)^2\tau_e\phi_{Rbb}^\alpha\left[1 + \frac{2}{3\pi^2}\frac{\tau_{a,B}}{\tau_e}\phi_p^{2\alpha}\right] \quad (3)$$

The complex modulus can be readily determined by inserting these results into eq A-11 in ref 1 with G_N replaced by $G_N\phi_p^{\alpha+1}$ for all terms except the constraint-release contribution, for which G_N is replaced by $G_N\phi_p$. The same model parameters, G_{Nf} = 0.6 MPa, M_{ef} = 4200 g/mol, and $\tau_{ef} = 7.4 \times 10^{-6}$ s, determined in the earlier 1,4-polyisoprene melt studies[1,6,17] are used for the predictions of symmetric and asymmetric star polymer solutions. We also make no effort to account for the small, but finite, polydispersity of the arms.

Storage and loss moduli of S101K, A_2B73K, and A_2B182K solutions are compared with the tube model predictions in Figures 5 and 6. It is apparent from Figure 5a that the model predictions are in uniformly good agreement with experimental data for S101K solutions with $1.0 \le \phi_p \le 0.6$. The crossover points at low and high frequencies are also correctly captured by the analysis. However, as shown in Figure 5b, large

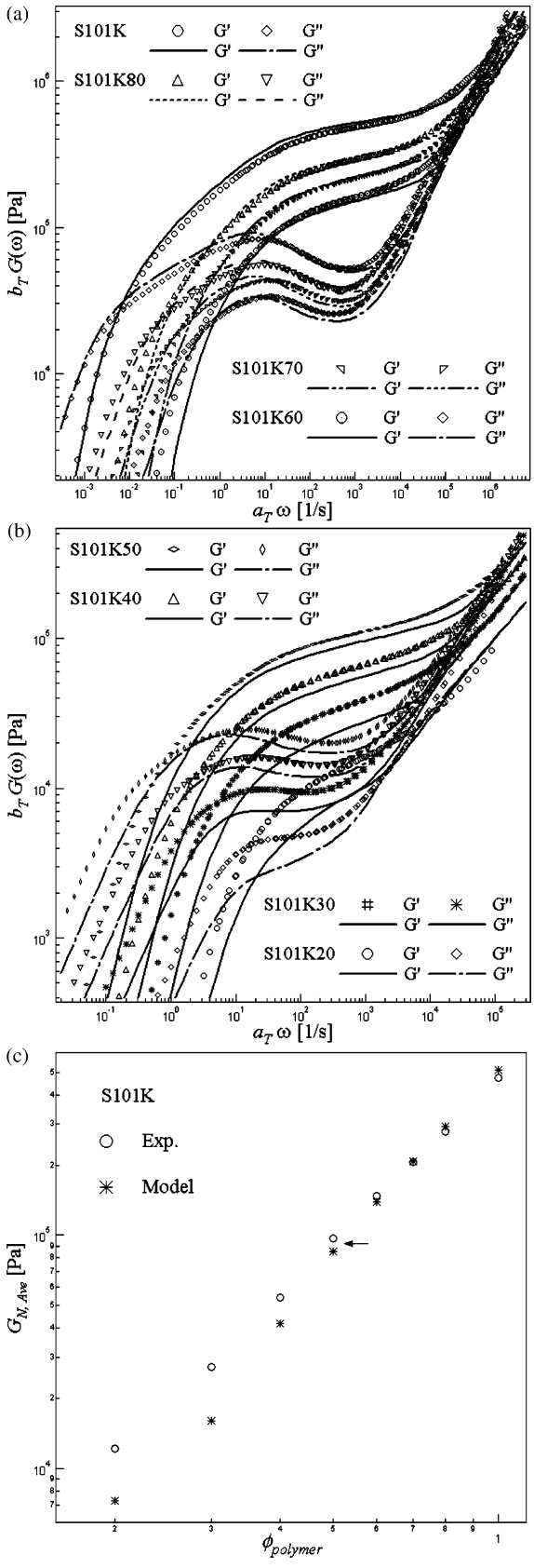

Figure 5. Comparison of experimental and theoretical (a) dynamic moduli, $G'(\omega)$ and $G''(\omega)$, of S101K solutions with $0.6 \le \phi_p \le 1.0$, (b) dynamic moduli, $G'(\omega)$ and $G''(\omega)$, of S101K solutions with $0.2 \le \phi_p \le 0.5$, and (c) plateau modulus of S101K solutions. Symbols are the measured data at T_{ref} = 28 °C, and lines are the tube model predictions with G_{Nf} = 0.6 MPa, M_{ef} = 4200 g/mol, and $\tau_{ef} = 7.4 \times 10^{-6}$ s.

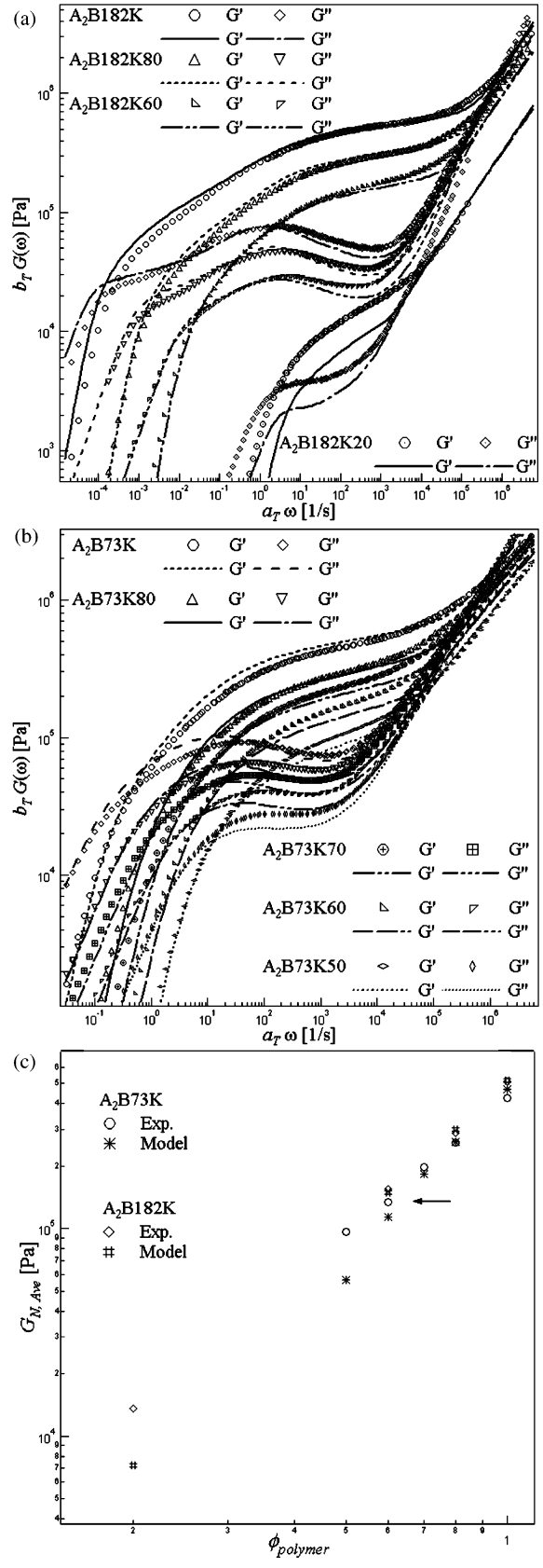

Figure 6. Comparison of experimental and theoretical (a) dynamic moduli, $G'(\omega)$ and $G''(\omega)$, of A_2B182K solutions with $0.2 \leq \phi_p \leq 1.0$, (b) dynamic moduli, $G'(\omega)$ and $G''(\omega)$, of A_2B73K solutions with $0.5 \leq \phi_p \leq 1.0$, and (c) plateau modulus of A_2B73K and A_2B182K solutions. Symbols are the measured data at $T_{ref} = 28$ °C, and lines are the tube model predictions with $G_{Nf} = 0.6$ MPa, $M_{ef} = 4200$ g/mol, and $\tau_{ef} = 7.4 \times 10^{-6}$ s.

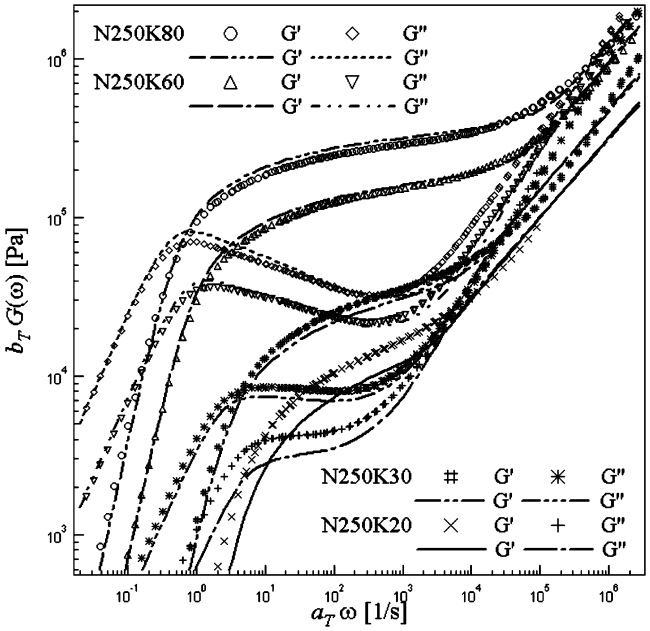

Figure 7. Comparison of experimental and theoretical dynamic moduli, $G'(\omega)$ and $G''(\omega)$, of N250K solutions. Symbols are the measured data at $T_{ref} = 28$ °C, and lines are the tube model predictions with $G_{Nf} = 0.6$ MPa, $M_{ef} = 4200$ g/mol, and $\tau_{ef} = 7.4 \times 10^{-6}$ s.

discrepancies between model predictions and experimental results emerge at lower polymer concentrations $0.5 \leq \phi_p \leq 0.2$. Useful hints about the source of this disagreement can be obtained by analyzing the apparent plateau moduli predicted by the theory and estimated (as the storage modulus value at the frequency where $G''(\omega)$ manifests a local minimum) from the data. The predicted plateau moduli are generally observed to deviate more from the experimental values as ϕ_p decreases. For example, the predicted $G_N(\phi_p)$ of S101K40 is 4.19×10^4 Pa, which is 77% of the value deduced from the experimental data. On the other hand, the $G_N(\phi_p)$ value for S101K70 obtained from the data is 2.06×10^5 Pa, which compares very well with the theoretical prediction of 2.08×10^5 Pa. Thus, below a polymer volume fraction of around 0.5, $M_{arm}/M_e(\phi_p) \approx 10$, the theory progressively overpredicts the effect of dilution on the entanglement network as ϕ_p decreases (see Figure 5c). Although the number of entanglements per arm at the onset of the deviations is relatively large, it is nonetheless close, $M_{arm}/M_e \approx 6$, to the degree of entanglement where dynamic dilution itself becomes and invalid assumption.[9] A similar observation was made for short, entangled star polybutadiene melts in our previous work.[17] It therefore seems reasonable to conclude that the discrepancies between experiment and theory at low star solution concentrations originates from the breakdown of the model framework used in our analysis. It is nonetheless also possible that the discrepancies stem from other, perhaps more subtle sources. For example, the predicted and measured crossover frequencies in the terminal relaxation region, $\omega_{crossover}$, are in noticeably better accord than the high-frequency crossover, $\omega_{c,H}$, for the same material. This effect is apparent from Figure 5b, for example, where the predicted and measured $\omega_{c,H}$ for S101K20 are seen to be quite far apart, yet the $\omega_{crossover}$ values are close. Given that the theoretical Θ-solvent scaling relationship for the entanglement hopping time, $\tau_e(\phi_p) = \tau_e/\phi_p^{8/3}$, was confirmed using the experimentally determined zero-shear viscosity, agreement between the measured and predicted $\omega_{crossover}$ is perhaps expected. The fact that $\omega_{c,H}$ is incorrectly captured in the lower concentration solutions, however, means

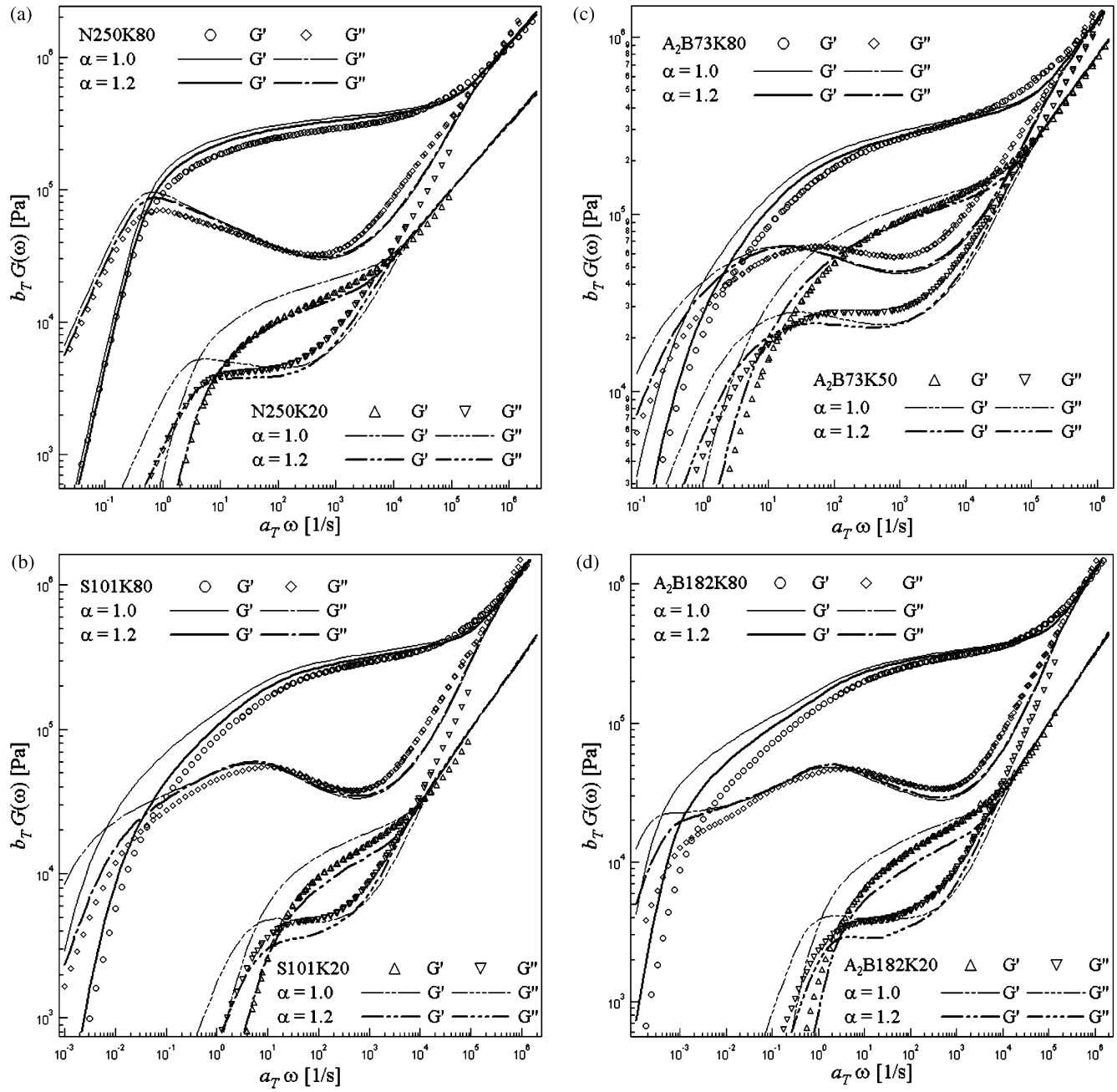

Figure 8. Comparison of experimental and theoretical moduli, $G'(\omega)$ and $G''(\omega)$, of (a) N250K20 and N250K80, (b) S101K20 and S101K80, (c) A_2B73K80 and A_2B73K50, and (d) A_2B182K80 and A_2B182K20. Symbols are the measured data at $T_{ref} = 28$ °C, and lines are the tube model predictions with $G_{Nf} = 0.6$ MPa, $M_{ef} = 4200$ g/mol, and $\tau_{ef} = 7.4 \times 10^{-6}$ s. The values of dilution exponent are $\alpha = 1.0$ and $\alpha = 1.2$.

that important details about relaxation dynamics on the scale of the entanglement segment are incorrectly described. Despite the fact that $M_{w,N4K}$ is lower than M_e for the melt, the closeness of the two values means that the possibility that the short chains may influence high-frequency relaxation dynamics of the stars in a qualitatively different manner than expected for a simple unentangled solvent cannot be ruled out. The contribution this type of behavior makes to the stress at lower ϕ_p could in principle be determined using a Rouse blend model for the high-frequency dynamics. These details are beyond the scope of the present work, and we will not pursue them any further.

Next we consider relaxation dynamics of asymmetric star polymer solutions. Figure 6a,b summarizes experimental $G'(\omega)$ and $G''(\omega)$ data (symbols) for solutions of A_2B182K and A_2-B73K at various polymer concentrations. The figures also provide theoretical predictions (lines) for the dynamic moduli of these solutions based on the earlier tube model analysis for asymmetric star melts,[1,6] extended to solutions in the same way as described earlier for symmetric stars. All parameters used in the analysis are also the same as those used for the symmetric star solutions. Again we make no effort to correct the model predictions for the small, but finite, polydispersity of the A and B arms.

It is apparent from Figure 6a,b that while there are quantitative discrepancies between the theoretical predictions and experimental results, the overall trends are captured reasonably well. At high asymmetric star polymer solution concentrations the quality of the theoretical predictions are in fact comparable to those for the melt. It is therefore tempting to conclude that solution properties of asymmetric star polymers can be predicted by simply extending melt models with rescaled (by dilution) entanglement spacings and entanglement Rouse times. As in

the case for the symmetric star polymers, however, more careful scrutiny of Figure 6b reveals a gradual worsening of the quality of the theoretical predictions as ϕ_p decreases. In particular, for symmetric and asymmetric stars, the theory predicts a much stronger effect of solution concentration on both moduli than observed experimentally. For example, if the plateau moduli estimated from experiment and theory are plotted against ϕ_p, as done in Figures 5c and 6c for symmetric and asymmetric stars, the theoretical predictions deviate noticeably from the experimental values for ϕ_p values around 0.5. Specifically, for $\phi_p = 0.6$, the predicted $G_N(\phi_p)$ of A_2B73K60 is 85% of the measured value, while the predicted $G_N(\phi_p)$ of A_2B182K60 is 96% of the measured value. It is also important to note that the number of entanglements per short arm for A_2B73K60 and A_2B182K60, $M_B/M_{ef}(\phi_p)$ or $M_B/M_e(\phi_p)$, is around 4, implying the assumed hierarchical relaxation mechanism should dominate relaxation dynamics for both materials. Indeed, if the characteristic time $\bar{\tau}$, at which the terminal behavior starts, is approximated as the reciprocal of $\omega_{crossover}$, the ratio of $\bar{\tau}_{A_2B182K60}/\bar{\tau}_{A_2B73K60}$ is around 283. On the other hand, the estimated reptation time of the linearlike backbone $\tau_{rep} = \tau_e(\phi_p)[2M_A/M_e(\phi_p)]^{3.4}$ yields $\tau_{rep,A_2B182K60}/\tau_{rep,A_2B73K60} \approx 22$, confirming that even four short arm entanglements are sufficient to produce a strong starlike contribution to the relaxation dynamics.

If the discrepancies between model predictions and data at lower symmetric or asymmetric star polymer concentrations, that is at lower degrees of arm entanglement, are indeed a consequence of breakdown of dynamic dilution, this effect should be limited to branched polymers. Figure 7 compare predicted and measured dynamic moduli for entangled solutions of a linear polyisoprene, N250K, at varying solution concentration. The model parameters used for these predictions are the same as those used for the symmetric and asymmetric star PI solutions. It is apparent from the figure that the model[24] quantitatively reproduces our experimental observations at high polymer concentrations. As the polymer concentration is lowered, however, qualitatively similar discrepancies to those observed for symmetric and asymmetric star polymer solutions become apparent. Specifically, the predicted moduli display similar frequency dependence as seen experimentally, but their magnitudes decrease too strongly with polymer concentration. At a solution concentration of 0.3, $M_L/M_e(\phi_p) \approx 13$, the solution plateau modulus estimated from the model is around 18% lower than that obtained from the experimental data, and at $\phi = 0.2$, $M_L/M_e(\phi_p) \approx 8$, the predicted modulus is around 30% lower. These discrepancies are smaller than, but comparable to, those observed for symmetric and asymmetric stars. They show that problems associated with breakdown of dynamic dilution (DD) or with the dynamic dilution assumption itself are not to blame because for the linear polymer DD is only active at the highest frequencies when contour length fluctuations dominate relaxation dynamics of the linear chains.

Our earlier discussion might suggest that $\alpha = 4/3$ is the only reasonable choice for polymer melts and solutions in Θ- or near-Θ-solvents. However, an important recent study concluded that somewhat smaller values of α are required to correctly fit experimental data for branched polymers using tube models similar to that employed in the present work.[25] Other studies have concluded that α values closer to unity are needed to correctly reproduce linear viscoelastic properties of bidisperse linear polymer blends.[26] Figure 8a−d illustrates the effect of α on stress relaxation dynamics for linear, star, and asymmetric star polymer solutions spanning the range of concentrations used in the study. It is apparent from all of these figures that while lower values of α can improve the overall quality of the theoretical predictions at particular polymer concentrations, and for a specific architecture, no choice of α simultaneously improves the theoretical predictions at both high and low polymer concentration for any architecture. In other words, the discrepancy between theory and experiment observed at the lower polymer concentrations cannot be remedied by changing the dilution exponent used in the analysis.

4. Conclusions

Linear viscoelastic behavior of a series of 1,4-polyisoprene linear, three-arm symmetric stars, and three-arm asymmetric star polymer melts and solutions is studied using a combination of experiment and theory to determine the effect of dilution by unentangled linear chains on the linear viscoelastic response in oscillatory shear flow. Solutions are created by blending the high molar mass polymer species with an unentangled 1,4-polyisoprene oligomer. By comparing the concentration dependence of the apparent plateau modulus estimated from linear viscoelastic data with expectations for the plateau modulus of an entangled polymer diluted by a Θ-solvent, we conclude that a single dilution exponent $\alpha = 4/3$ is consistent with the experimental data, irrespective of polymer architecture.

A tube-based model used successfully in an earlier study to predict linear viscoelastic properties of entangled polymer melts with a range of architectures[1,6] (including linear, T- and Y-shaped asymmetric stars, H-shaped, pom-poms, and combs) is employed in the present work to evaluate the model framework for entangled polymers possessing a wider range of entanglement densities. We find that by simply rescaling the three model parameters, M_e, τ_e, and G_N, to their respective Θ-solution values, $M_e(\phi_p) = M_e/\phi_p^{4/3}$, $\tau_e(\phi_p) = \tau_e[M_e(\phi_p)/M_e]^2 = \tau_e/\phi_p^{8/3}$, and $G_N(\phi_p) = G_N\phi_p^{7/3}$, the analysis yields dynamic moduli for concentrated polymer solutions that are of comparable quality to those deduced in the earlier work for melts. In particular, using the same model parameters employed in the earlier work for PI melts, linear viscoelastic properties of entangled linear, symmetric stars, and asymmetric stars polymer solutions are essentially quantitatively reproduced at polymer concentrations above 40%−50%. At lower polymer concentrations, we find that the model predictions systematically deviate from the experimental data, with the model overpredicting the effect of solvent dilution on the magnitude of the dynamic moduli. We explore several potential sources of these errors, including breakdown of dynamic dilution, nonuniversality of the dilution exponent, and complex local "solvent" dynamics, and find that none explain the model failings at low polymer concentrations.

Acknowledgment. Financial support from the National Science Foundation (Grant DMR0551185) is gratefully acknowledged.

References and Notes

(1) Lee, J. H.; Fetters, L. J.; Archer, L. A. *Macromolecules* **2005**, *38*, 4484.
(2) Milner, S. T.; McLeish, T. C. B. *Macromolecules* **1997**, *30*, 2159.
(3) McLeish, T. C. B.; et al. *Macromolecules* **1999**, *32*, 6738.
(4) Daniels, D. R.; McLeish, T. C. B.; Crosby, B. J.; Young, R. N.; Fernyhough, C. M. *Macromolecules* **2001**, *34*, 7025.
(5) Frischknecht, A. L.; Milner, S. T.; Pryke, A.; Young, R. N.; Hawkins, R.; McLeish, T. C. B. *Macromolecules* **2002**, *35*, 4801.
(6) Lee, J. H.; Fetters, L. J.; Archer, L. A. *Macromolecules* **2005**, *38*, 10763.
(7) Marrucci, G. *J. Polym. Sci., Polym. Phys. Ed.* **1985**, *23*, 159.
(8) Ball, R. C.; McLeish, T. C. B. *Macromolecules* **1989**, *22*, 1911.

(9) Frischknecht, A. L.; Milner, S. T. *Macromolecules* **2000**, *33*, 9764.
(10) Clarke, N.; Roger Colley, F.; Collins, S. A.; Hutchings, L. R.; Thompson R. L. *Macromolecules* **2006**, *39*, 1290.
(11) Daniels, D. R.; McLeish, T. C. B.; Kant, R.; Crosby, B. J.; Young, R. N.; Pryke, A.; Allgaier, J.; Groves, D. J.; Hawkins, R. J. *Rheol. Acta* **2001**, *40*, 403.
(12) Colby, R. H.; Rubinstein, M. *Macromolecules* **1990**, *23*, 2753.
(13) Rubinstein, M.; Colby, R. H. *Polymer Physics*; Oxford University Press: Oxford, 2003.
(14) Miros, A.; Vlassopoulos, D.; Likhtman, A. E.; Roovers, J. *J. Rheol.* **2003**, *47*, 163.
(15) Juliani; Archer, L. A. *Macromolecules* **2002**, *35*, 6953. Juliani; Archer, L. A. *Macromolecules* **2002**, *35*, 10048.
(16) Archer, L. A.; Juliani *Macromolecules* **2004**, *37*, 1076.
(17) Lee, J. H.; Fetters, L. J.; Archer, L. A.; Halasa, A. F. *Macromolecules* **2005**, *38*, 3917.
(18) Tanaka, Y.; Takeuchi, Y.; Kobayashi, M.; Tadokoro, H. *J. Polym. Sci., Part A-2* **1971**, *9*, 43.
(19) Adam, M.; Delsanti, M. *J. Phys. (Paris)* **1983**, *45*, 1513.
(20) Pearson, D. S. *Rubber Chem. Technol.* **1987**, *60*, 439.
(21) Colby, R. H.; Fetters, L. J.; Funk, W. G.; Graessley, W. W. *Macromolecules* **1991**, *24*, 3873.
(22) Tao, H.; Lodge, T. P.; von Meerwall, E. D. *Macromolecules* **2000**, *33*, 1747.
(23) Wang, S. F.; von Meerwall, E. D.; Wang, S. Q.; Halasa, A.; Zhou, J. P.; Quirk, R. P. *Macromolecules* **2004**, *37*, 1641.
(24) Milner, S. T.; McLeish, T. C. B. *Phys. Rev. Lett.* **1998**, *81*, 725.
(25) Kapnistos, M.; Vlassopoulos, D.; Roovers, J.; Leal, L. G. *Macromolecules* **2005**, *38*, 7852.
(26) Park, S. J.; Larson, R. G. *Macromolecules* **2004**, *37*, 597.

MA061151A